Supporting Information: Self-Assembly and Hydrogelation of an Amyloid Peptide Fragment

Marta J. Krysmann, Valeria Castelletto, Antonios Kelarakis and Ian W. Hamley, Rohan A. Hule and Darrin J. Pochan

1. UV/Vis Absorption Spectroscopy

The Chirascan spectropolarimeter was used in UV absorption mode, with the sample in a 1.0 cm quartz cuvette. The absorbance was measured for water and solutions of KLVFF in water (0.01 and 0.000625% wt). The spectra were recorded from 180 to 400 nm at room temperature and the background was subtracted. Fig. S1 shows the resulting spectra.

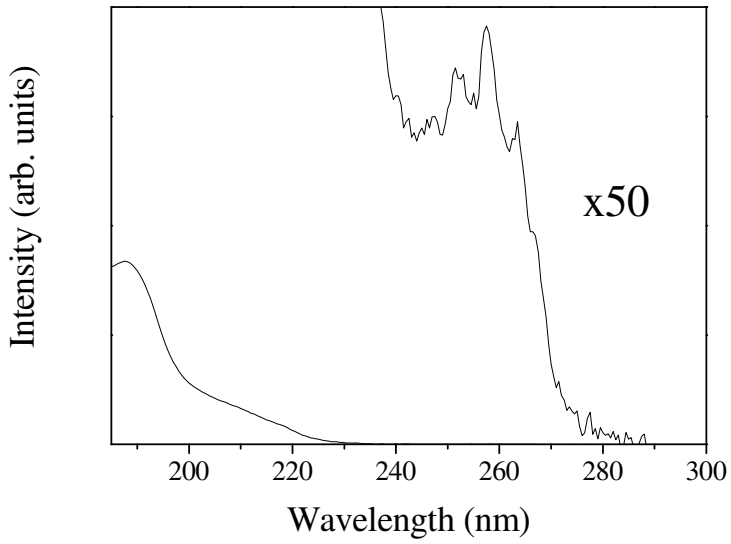

Supplementary Figure S1. UV absorption spectra showing aromatic interactions in KLVFF. The data in the 180-230 nm range were measured for a 0.000625 wt.% sample, that on the expanded scale for 240-290 nm were measured for a 0.01 wt.% sample.

2. Full FTIR and Raman Spectra

FTIR spectroscopy. The full FTIR spectrum was measured as described in the manuscript.

Raman spectroscopy. Raman spectra of lyophilised peptide were recorded by a Perkin-Elmer GX Fourier transform spectrometer, equipped with an excitation source of a diode pumped Nd-YAG laser at 1064 cm^{-1}. The laser power was set at 200 mW and the resolution was 4 cm^{-1}. Spectra were monitored from 3500 to 500 cm^{-1} with an interval 2 cm^{-1} at room temperature. All spectra were analyzed using GRAMS/32 data analysis software.

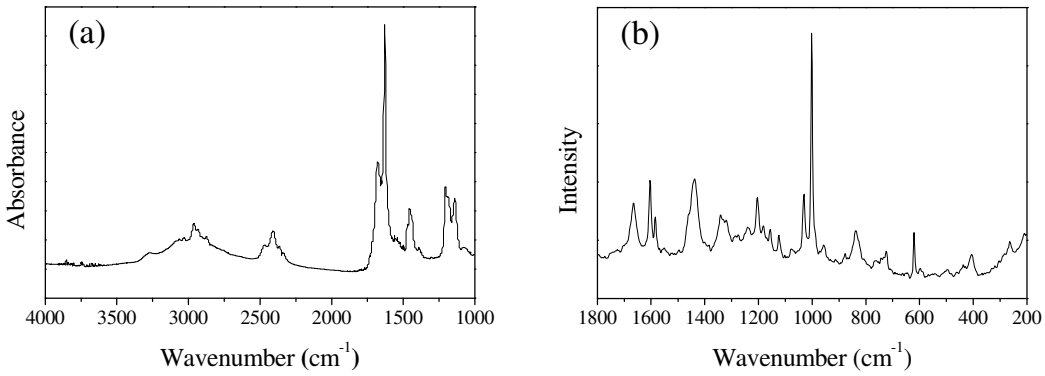

Supplementary Figure S2. (a) Full FTIR spectrum for a sample dried from 3 wt.% KLVFF in D_2O (Fig.3(b) contains an expanded view of the amide I region of this spectrum). The solvent spectrum has been subtracted from the spectra of the peptide solutions. (b) Raman of lyophilised KLVFF.

The full FTIR spectrum for a dried sample is shown in Fig. S2a. Additional peaks were located in the amide A band at 3274 cm^{-1}. An absorption peak at 3030 cm^{-1} was due to stretching vibration from the benzene rings. A peak at 2962 cm^{-1} was due to the CH_3 vibration. The peak at 2936 cm^{-1} was assigned to the CH_2 asymmetric stretching bands while the peak at 2874 cm^{-1} was due to the CH_3 symmetric stretching bands. The peaks at 1673 and 1629 cm^{-1} were assigned with the amide I band and the peak at 1455 cm^{-1} was signed to the amide II band. The CN and CO stretching bands correspond respectively to peaks at 1204 and 1139 cm^{-1}. [1, 2]

It was possible to obtain further information on secondary structure using Raman spectroscopy on dried samples (Fig. S2b). In the analysis we only consider the Raman spectrum from 400 to 1800 cm^{-1} since most of the information in this region relates to secondary structure and the side chain in KLVFF. In Raman spectroscopy the most useful vibrational modes sensitive to peptide conformation are amide I which involves mainly C=O stretching vibrations and amide III which has contributions from both C-N stretching and N-H in-plane bending vibrations. We observed a broad peak at 1665 cm^{-1}, in the amide I region, which can be assigned to disordered structure[3, 4] or alternatively to β-sheet and type II β-turn structures.[5, 6] The main amide I band is accompanied by a weaker shoulder at 1670-1690 cm^{-1} which can be assigned to β-sheet structure, again with a possible contribution from β turns.[5, 6] Recent studies combining Raman optical activity experiments and conventional Raman spectroscopy indicate that features in the range 1665-1680 cm^{-1} correspond to β-sheet structures.[7, 8]

In the amide III region, several peaks were observed at 1232, 1272, 1280, 1319 cm^{-1}. Peaks in the range 1260-1340 cm^{-1} were assigned to β-turn structures.[5, 7] The peak at 1232 cm^{-1} may be assigned to β-sheet structure.[3, 5, 7] The observed peaks together indicate a structure based on β-sheets coexisting with with β-turns. Bands assigned to phenylalanine aromatic side chains were observed at 620, 1001, 1031 (the latter two form a strong doublet), 1204, 1585, 1603 cm^{-1} while peaks at 724, 952, 1460 cm^{-1} were assigned to aliphatic chains.[9-11]

3. Congo Red Staining

Staining and Imaging of Stained Sample. Dried samples of KLVFF were stained with freshly prepared and filtered Congo Red solution (a solution of 0.5 g Congo red

powder suspended in 80 mL of absolute EtOH was combined with 2 g of sodium chloride dissolved in 20 mL double-distilled deionized water)[12] and placed onto glass microscope slide and dried. Images of sample placed between crossed polarised were obtained with an Olympus CX-41 microscope. An example is shown in Fig. S3.

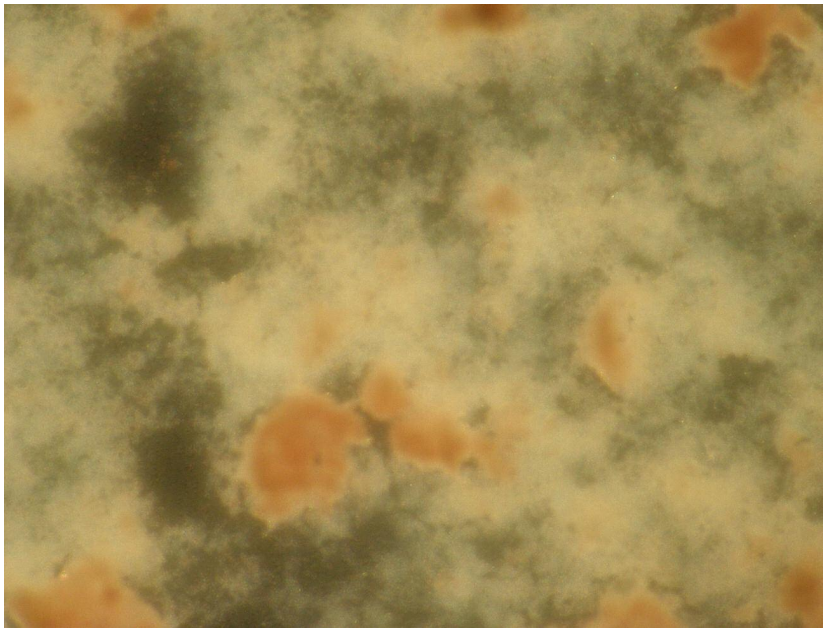

Supplementary Figure S3. Polarized optical microscopy image of KLVFF stained with Congo Red

4. Negative Stain TEM

Transmission electron microscopy (TEM) was performed in the Centre for Advanced Microscopy at the University of Reading. A Philips CM20 transmission electron microscope, operated at 80kV, was used to study and record images of KLVFF solutions. A droplet of the sample (1% wt in PBS and 3% wt in water) was placed on polyvinyl formal grids (Agar Scientific, UK), stained with methylamine tungstate (1% wt) (Agar Scientific, UK) and dried. Fibril dimensions were subjected to statistical analysis in regions of the images using Scandium software.

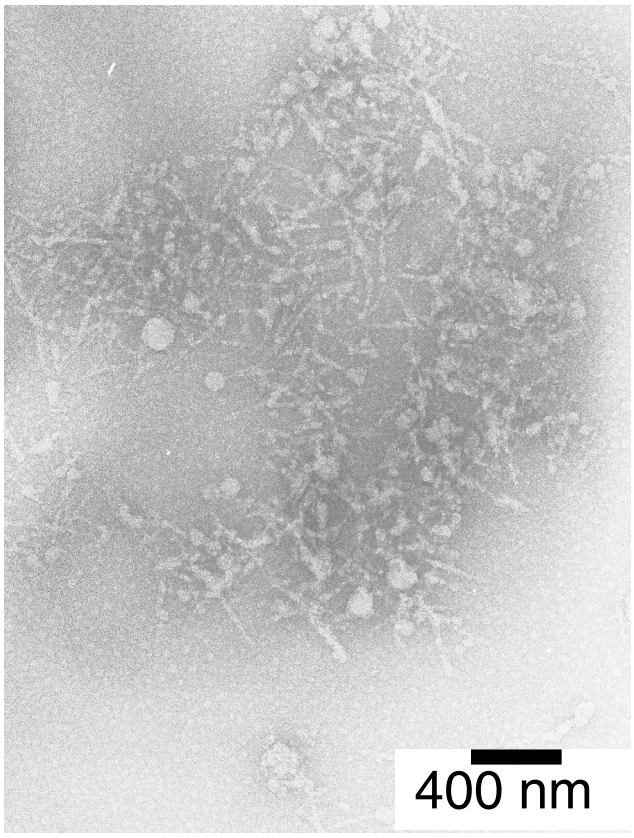

Supplementary Figure S4. Conventional TEM image of KLVFF negatively stained with uranyl acetate for a sample dried from 3 wt.% aqueous solution after incubation at 60 ^{o}C for 3 hr.

The micrograph shows large globules coexisting with large irregular filamentous aggregates. This image was obtained for a 3 wt.% sample incubated for 3 hrs at 60 ^{o}C in an attempt to enhance fibrillisation. Micrographs that are very similar to Supplementary Figure S4 and that show the coexistence of large globular objects and fibrous bundles have previously been observed by conventional TEM for the full Aβ40 or Aβ42 peptide,[13, 14] or fragments of it,[15, 16] as well as other amyloid-forming proteins.[17, 18]

5. Small-Angle X-ray Scattering

The scattering intensity from a dilute solution of homogeneous infinite solid cylinders with polydisperse cross section can be written[19]

$$I(q) \propto \int_0^\infty \exp\left[(r - r_c)^2 / 2\sigma^2\right] \left[J_1^2(qr)/q^3 r^2\right] \, dr + BG \qquad (1)$$

Here r_c is the average cylinder radius, $(\sigma/r_c)\times 100$ is the percent of polydispersity in r_c. BG in Eq. 1 is the background, given by

$$BG = A + Bq^{-C} \qquad (2)$$

The fitting parameters of our model were r_c = 58 Å, σ = 4.5 Å [$(\sigma/r_c)\times 100$ = 8%], A= $1.0\text{x}10^{-2}$, B= $1.5\text{x}10^{-4}$ and C= -1.6 (close to C = -1 expected for infinite cylinders with a smooth surface).[19]

REFERENCES

1. Stuart, B., *Biological Applications of Infrared Spectroscopy*. Wiley: Chichester, 1997.

2. Lin, S.-Y.; Chu, H.-L., Fourier transform infrared spectroscopy used to evidence the prevention of β sheet formation of amyloid β(1-40) pepride by short amyloid fragment. *International Journal of Biological Macromolecules* **2003,** 32, 173-177.
3. Spiro, T. G.; Gaber, B. P., Laser Raman scattering as a probe of protein structure. *Annual Review of Biochemistry* **1977,** 46, 553-572.
4. Pelton, J. T.; McLean, L. R., Spectroscopic methods for analysis of protein secondary structure. *Analytical Biochemistry* **2000,** 277, 167-176.
5. Bandekar, J.; Krimm, S., Vibrational analysis of peptides, polypeptides, and proteins: Characteristic amide bands of β-turns. *Proceedings of the National Academy of Sciences of the United States of America* **1979,** 76, (2), 774-777.
6. Benaki, D. C.; Aggeli, A.; Chryssikos, G. D.; Yiannopoulos, Y. D.; Kamitsos, E. I.; Brumley, E.; Case, S. T.; Boden, N.; Hamodrakas, S. J., Laser-Raman and FT-IR spectroscopic studies of peptide-analogues of silkmoth chorion protein segments. *International Journal of Biological Macromolecules* **1998,** 23, (1), 49-59.
7. McColl, I. H.; Blanch, E. W.; Gill, A. C.; Rhie, A. G. O.; Ritchie, M. A.; Hecht, L.; Nielsen, K.; Barron, L. D., A new perspective on β-sheet structures using vibrational Raman optical activity: From poly(L-lysine) to the prion protein. *Journal of the American Chemical Society* **2003,** 125, 10019-10026.
8. Barron, L. D.; Blanch, E. W.; Hecht, L., Unfolded proteins studied by Raman optical activity. *Advances in Protein Chemistry* **2002,** 62, 51-90.
9. Overman, S. A.; Thomas, G. J., Virus Structure by Laser Raman-Spectroscopy .45. Raman-Spectroscopy of the Filamentous Virus Ff (Fd, Fl, M13) - Structural Interpretation for Coat Protein Aromatics. *Biochemistry* **1995,** 34, (16), 5440-5451, erratum 7780.

10. Overman, S. A.; Thomas, G. J., Raman markers of nonaromatic side chains in an alpha-helix assembly: Ala, Asp, Glu, Gly, Ile, Leu, Lys, Ser, and Val residues of phage fd subunits. *Biochemistry* **1999,** 38, (13), 4018-4027.
11. Podstawka, E.; Borszowska, R.; Grabowska, M.; Drag, M.; Kafarski, P.; Proniewicz, L. M., Investigation of molceular structures and adsorption mechanisms of phosphonodipeptides by surface-enhanced Raman, Raman, and infrared spectroscopies. *Surface Science* **2005,** 599, 207-220.
12. Nilsson, M. R., Techniques to study amyloid fibril formation in vitro. *Methods* **2004,** 34, 151-160.
13. Bitan, G.; Kirkitadze, M. D.; Lomakin, A.; Vollers, S. S.; Benedek, G. B.; Teplow, D. B., Amyloid b-protein (Ab) assembly: Ab40 and Ab42 oligomerize through distinct pathways. *Proceedings of the National Academy of Sciences of the United States of America* **2003,** 100, (1), 330-335.
14. Chafekar, S. M.; Malda, H.; Merkx, M.; Meijer, E. W.; Viertl, D.; Lashuel, H. A.; Baas, F.; Scheper, W., Branched KLVFF tetramers strongly potentiate inhibition of β-amyloid aggregation. *ChemBioChem* **2007,** 8, 1857-1864.
15. Tjernberg, L. O.; Callaway, D. J. E.; Tjernberg, A.; Hahne, S.; Lilliehöök, C.; Terenius, L.; Thyberg, J.; Nordstedt, C., A molecular model of Alzheimer amyloid β-peptide fibril formation. *Journal of Biological Chemistry* **1999,** 274, (18), 12619-12625.
16. Kallberg, Y.; Gustafsson, M.; Persson, B.; Thyberg, J.; Johansson, J., Prediction of amyloid fibril-forming proteins. *Journal of Biological Chemistry* **2001,** 276, (16), 12945-12950.

17. Hurshman, A. R.; White, J. T.; Powers, E. T.; Kelly, J. W., Transthyretin aggregation under partially denaturing conditions is a downhill polymerization. *Biochemistry* **2004,** 43, 7365-7381.

18. Bader, R.; Bamford, R.; Zurdo, J.; Luisi, B. F.; Dobson, C. M., Probing the mechanism of amyloidogenesis through a tandem repeat of the PI3-SH3 domain suggests a generic model for protein aggregation and fibril formation. *Journal of Molecular Biology* **2006,** 356, (1), 189-208.

19. Glatter, O.; Kratky, O., *Small Angle X-ray Scattering*. Academic: London, 1982.